Dielectrophoresis of Micro/Nano Particles Using Curved Microelectrodes

Khashayar Khoshmanesh [1*], Francisco J. Tovar-Lopez [2], Sara Baratchi [3], Chen Zhang [4], Aminuddin A. Kayani [2], Adam F. Chrimes [2], Saeid Nahavandi [1], Donald Wlodkowic [5], Arnan Mitchell [2], Kourosh Kalantar-zadeh [2]

[1] Centre for Intelligent Systems Research, Deakin University, Waurn Ponds, Australia
[2] School of Electrical and Computer Engineering, RMIT University, Melbourne, Australia
[3] Department of Biochemistry and Molecular Biology, Monash University, Clayton, Australia
[4] Ian Wark Research Institute, University of South Australia, Mawson Lakes, Australia
[5] The BioMEMS Research Group, School of Chemical Sciences, University of Auckland, New Zealand

ABSTRACT

Dielectrophoresis, the induced motion of polarisable particles in non-homogenous electric field, has been proven as a versatile mechanism to transport, immobilise, sort and characterise micro/nano scale particle in microfluidic platforms. The performance of dielectrophoretic (DEP) systems depend on two parameters: the configuration of microelectrodes designed to produce the DEP force and the operating strategies devised to employ this force in such processes. This work summarises the unique features of curved microelectrodes for the DEP manipulation of target particles in microfluidic systems. The curved microelectrodes demonstrate exceptional capabilities including (i) creating strong electric fields over a large portion of their structure, (ii) minimising electro-thermal vortices and undesired disturbances at their tips, (iii) covering the entire width of the microchannel influencing all passing particles, and (iv) providing a large trapping area at their entrance region, as evidenced by extensive numerical and experimental analyses. These microelectrodes have been successfully applied for a variety of engineering and biomedical applications including (i) sorting and trapping model polystyrene particles based on their dimensions, (ii) patterning carbon nanotubes to trap low-conductive particles, (iii) sorting live and dead cells based on their dielectric properties, (iv) real-time analysis of drug-induced cell death, and (v) interfacing tumour cells with environmental scanning electron microscopy to study their morphological properties. The DEP systems based on curved microelectrodes have a great potential to be integrated with the future lab-on-a-chip systems.

1. INTRODUCTION

Dielectrophoresis, the induced motion of neutral polarisable particles in a non-uniform electric field, has been proven as a versatile mechanism to transport, sort, accumulate and characterise the suspended micro/nano scale particles in microfluidic systems. The integration of dielectrophoretic (DEP) systems into microfluidics allows for the inexpensive, rapid, sensitive, selective and label-free detection and analysis of target particles, as comprehensively reviewed in [1-5].

Subjecting a polarisable particle such as cells to an electric field makes it polarised, and induces electrical charges on the interface of particle/medium. The induced charges make up dipoles which are aligned parallel to the applied filed. In a uniform electric field, each half of the dipole experiences balanced Columbic forces, resulting in a net zero force applied on the particle. Conversely, in a non-uniform electric field, each half of the dipole experiences imbalanced Columbic forces, resulting in a net force applied on the particle. The particle can be pushed towards or away from the regions of strong electric field depending on the particle is more/less polarisable than the suspending medium, and such a movement is called dielectrophoresis [1].

* Corresponding author: Khashayar.khoshmanesh@deakin.edu.au

Dielectrophoresis offers the controllable, selective and accurate manipulation of suspended particles. Unlike electrophoresis, which relies on the charge-to-size ratio of particles, dielectrophoresis relies on their dielectric properties [6]. The dielectric properties in turn, represent the structural, morphological and chemical characteristics of the particle and hence, enable the dielectrophoresis for the more selective and sensitive manipulation of particles [7].

The microelectrodes, which are the heart of DEP systems, are offered in a variety of configurations including: parallel or interdigitated [8], castellated [9], oblique [10], curved [11], quadrupole [12], microwell [13], matrix [14], extruded [15], top-bottom patterned [16], sidewall patterned [17], insulator-based or electrodeless [18], and contactless [19], as reviewed in [2].

In this paper, we demonstrate the successful application of curved microelectrodes for a variety of engineering and biomedical applications, including: (i) sorting and trapping model polystyrene particles based on their dimensions, (ii) patterning carbon nanotubes to trap low-conductive particles at high frequencies and high medium conductivities, (iii) sorting live and dead cells based on their dielectric properties, (iv) real-time analysis of drug-induced cell death, and (v) interfacing tumour cells with environmental scanning electron microscopy to study their morphological properties. The DEP systems based on curved microelectrodes have a great potential to be integrated with the future lab-on-a-chip systems.

2. SPECIFICATIONS OF CURVED MICROELECTRODES

Figure 1A presents the geometric details of curved microelectrodes with the trace width of 50 μm, the minimum gap of 40 μm between the opposite microelectrodes, and the 1000 μm spacing between the sequential microelectrode pairs. The microelectrodes are energised through pads of 6×2.25 mm patterned on the both sides. The substrate is a glass slide of 75×25.5×1 mm that supports five pairs of microelectrodes on its surface. To fabricate the microelectrodes, a thin film of chrome was deposited on a glass substrate with a thickness of 500 Å to serve as adhesive layer followed by a gold film with a thickness of 1500 Å using the electron beam evaporation process. The pattern of the microelectrodes was then defined using conventional photolithography techniques. The copper wires were bonded to the microelectrode pads, using silver-based epoxy glue [11].

Figure 1B shows the contours of electric field produced at the bottom surface of the microchannel, indicating the steady increase of electric field along the structure until reaching a peak at the tips. The smooth increase of electric field maximises the effective length of structure while minimising high temperatures, electro-thermal vortices and undesired motions at the tips [11]. Figure 1C shows the vectors of attractive DEP force along the curved microelectrodes. Strong DEP forces near the tip region facilitate the trapping or repelling of suspended particles across the delta-shaped region between the microelectrodes [20].

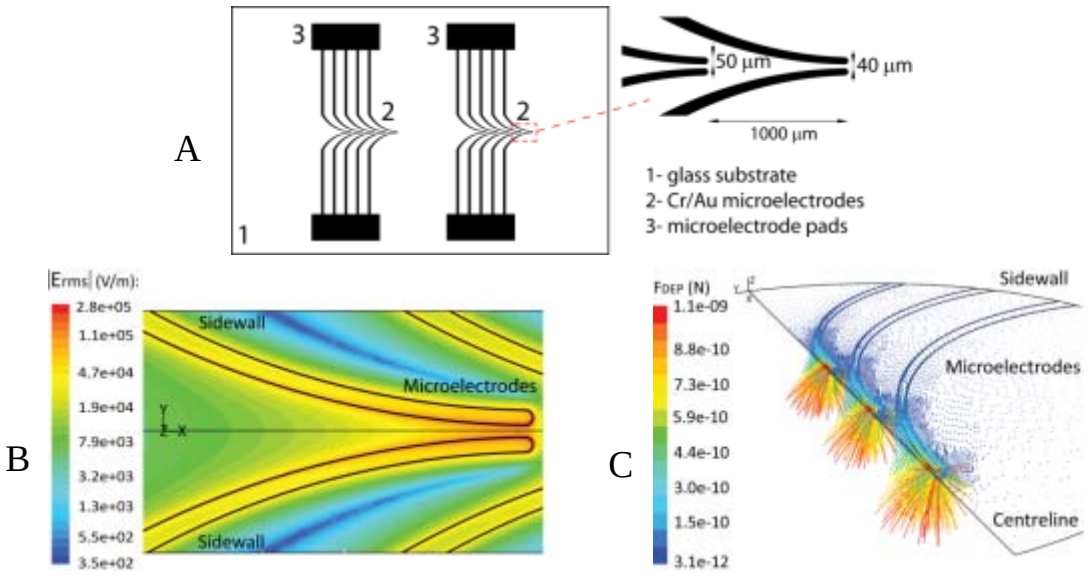

Figure 1. Details of curved microelectrodes: (A) Geometrical details [11], (B) Contours of electric filed generated at 10 V, (C) Vectors of DEP force (in attractive mode) generated at 10 V obtained by numerical simulations [20].

3. RESULTS AND DISCUSSIONS

3.1. Sorting and trapping model polystyrene particles based on their dimensions

Figure 2A shows the application of curved microelectrodes in a flow-through configuration. The microchannel is fabricated from polydimethylsiloxane (PDMS) with a width of 600 µm and a height of 80 µm. Polystyrene particles of 1, 6 and 15 µm were applied to the system while the flow rate and conductivity of the buffer were set to 0.2 µlit/min and 2×10^{-4} S/m and the magnitude and frequency of the applied signal were set to 15 V and 200 kHz. At this frequency, the 1 µm particles exhibited positive DEP response while the 6 and 15 µm particles behaved oppositely (Figure 2B). Under those conditions, it was expected to trap the 1 µm particles between the microelectrodes while repelling the larger particles [21].

Figures 2C shows the response of particles at the second microelectrode pair. The 1 µm particles were trapped along the microelectrodes while most of them were accumulated at the tips due to the presence of strong electric field gradients. The particles, which still remained in the flow, gradually lost their heights under the positive DEP-z force until being trapped by the next pairs. Alternatively, the 6 µm particles were repelled towards the sidewalls and simultaneously levitated at higher heights. The consequent microelectrode pairs stabilised the location of particles and led to the formation of thick strips close to the sidewalls. Finally, the 15 µm particles were repelled towards the sidewalls. Most of the particles were retained behind the second microelectrode pair. The particles still suspended in the flow passed through the microchannel in a zigzag motion until being filtered by the next pairs.

The trapping efficiency of trapped 1 µm particles and retained 15 µm particles were measured as 79±3% and 85±4%, respectively applied a standard cell counting chamber slide (Neubauer hemocytometer), while the 6 µm particles which freely passed the microelectrodes were collected at the outlet with a yield and enrichment factor of 93±3% and 2.5, respectively.

The unique capabilities of curved microelectrodes to guide the micro/nano particles along the desired trails of the microchannel has been applied to develop novel optufluidic systems, in which the optical properties of the medium can be tuned by guiding SiO_2 nanoparticles along the predetermined locations of the microchannel [22-23] and also to develop a microfluidic-Raman spectroscopy system to map the spatial concentration of WO_3 nanoparticles within the microchannel [24].

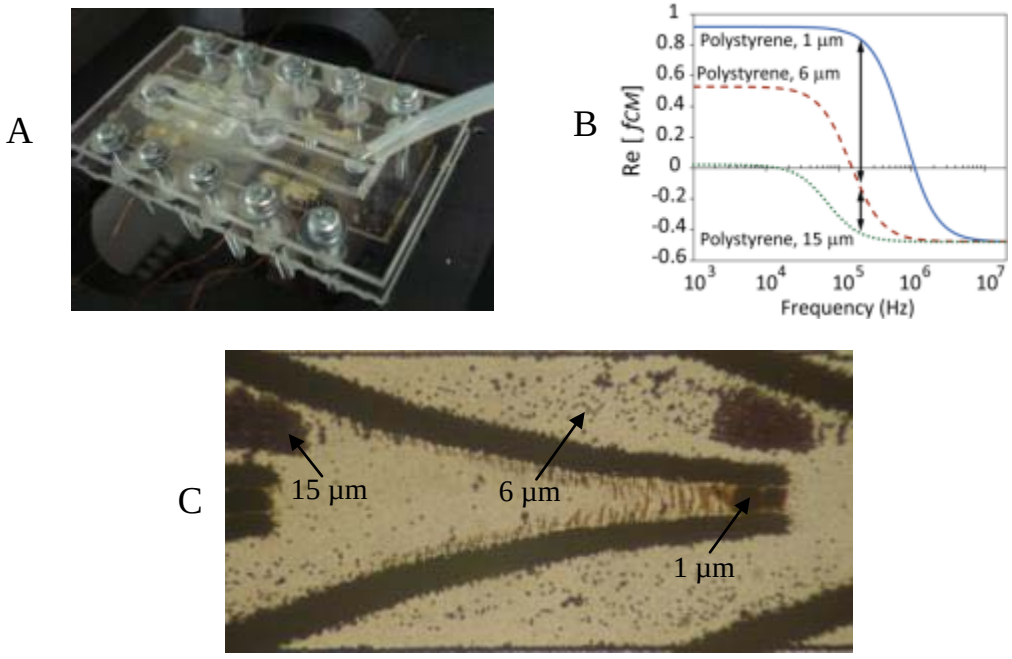

Figure 2. Sorting and trapping model polystyrene particles using curved microelectrodes: (A) The DEP device in a flow through configuration, (B) DEP response of 1, 6 and 15 µm particles, and (C) The separation of particles shown at the second microelectrode pair [21].

3.2. Patterning carbon nanotubes to trap low-conductive particles

Figure 3A shows the response of 6 µm COOH-coated polystyrene particles to the DEP field. The magnitude and frequency of the applied signal were set to 15 V and 20 MHz while the flow rate and conductivity of the flow were set to 0.5 µlit/min and 5×10^{-4} S/m, respectively. Approaching the first microelectrode, the neighbouring particles were attracted to each other forming pearl chains under the increasing electric field. The particles exhibited negative DEP behaviour and were repelled from the microelectrode tips to create a particle-free region along the centreline (Figure 3D) [25].

Figure 3B shows the response of Pt/N-CNTs to the first microelectrode pair of the system after 3 minutes. The magnitude of the applied signal was decreased to 12.5 V to decelerate the deposition of Pt/N-CNTs. The Pt/N-CNTs exhibited positive DEP behaviour due to their high conductivity and were trapped between the microelectrodes. The density of the patterned Pt/N-CNTs followed the contours of the electric field and reached a peak at the tips. The patterning process was self-regulating and stopped when a large amount of patterned Pt/N-CNTs bridged between the opposite pairs and weakened the electric field in 5-7 minutes.

Figure 3C shows the trapping of 6 µm COOH-coated polystyrene particles by the patterned Pt/N-CNTs. The Pt/N-CNTs were applied to the system and were allowed to pattern between the microelectrodes for 3-4 minutes to ensure that the Pt/N-CNTs deposited at the entry region had grown enough to cover a large portion of the microchannel. Then, the particles were injected to the reservoir. The Pt/N-CNTs, which still remained in the reservoir coated the surface of the particles and increased their overall conductivity and permittivity, such that they exhibited positive DEP response (Figure 3D). This process was completed at the microchannel, where the suspended Pt/N-CNTs and particles had more chance to interact. The patterned Pt/N-CNTs induced a strong electric field at the entry of the first microelectrode pair, which accelerated the formation of pearl chains between the neighbouring Pt/N-CNT-coated particles and their entrapment [25].

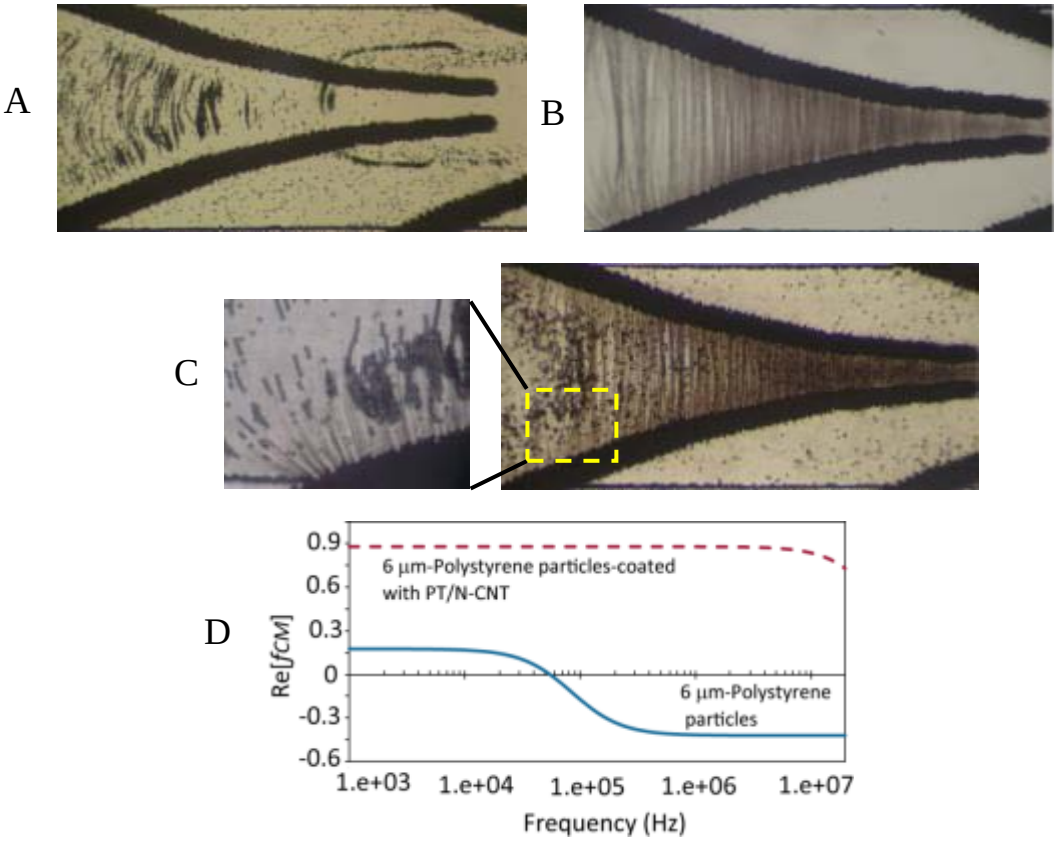

Figure 3. Integration of CNTs to DEP system to trap low-conductive particles: (A) Repelling of 6 µm COOH-coated polystyrene particles, (B) Patterning of Pt/N-CNTs between the microelectrodes, (C) Trapping of Pt/N-CNT-coated particles, and (D) Distinct response of 6 µm COOH-coated polystyrene particles with/without Pt/N-CNT [25].

3.3. Sorting live and dead yeast cells based on their dielectric properties

Sorting cells based on their physical or biochemical properties is essential for diagnosing diseases. The most widely used techniques for cell sorting are density gradient cell sorting [26], immunochemical conjugation [27-28], fluorescent-activated cell sorting (FACS) [29-30] and magnetic-activated cell sorting (MACS) [31]. The distinctive capabilities of dielectrophoresis to sort the cells based on their dielectric properties enables a new generation of dielectrophoretic-activated cell sorters (DACS).

Figure 4 shows the sorting of live and dead (methanol treated) yeast cells under the combined effect of DEP and hydrodynamic forces. The microchannel is fabricated from PDMS with a width of 1000 μm and a height of 80 μm. Trypan blue was used to distinguish between the live and dead cells, which in turn increased the electrical conductivity of LEC buffer to 0.14 S/m. At this medium conductivity, the live cells exhibited positive DEP response at frequencies higher than 2 MHz while the dead cells exhibited negative DEP response over the entire frequency range (Figure 4A). Applying an AC signal at 20 MHz facilitates the separation of live and dead cells at this medium conductivity [32].

The flow rate was set to 0.6 μlit/min while the magnitude of AC signal was set to 12.5 V to diminish the electro-convective motions at the tips. Figure 4B shows the separation of live and dead yeast cells in the above conditions. The live cells were pushed towards the microelectrode edges under the influence of attractive DEP force. Once a live cell attached to the microelectrodes, it attracted more cells to its free end. This formed a dense layer of live cells between the microelectrodes, especially at the regions close to the tip region. Interestingly, the cells were not immobilised at the tips due to disturbing presence of electro-convective vortices (Figure 4B). Conversely, the dead cells were decelerated and funnelled between the microelectrodes. Approaching the tips the chains were broken, the dead cells were levitated to higher heights and most of them pushed towards the sidewalls. A small portion of dead cells were focused along the centreline to avoid the tip region.

The magnified image shows the portion of dead (stained) to live (non-stained) cells along the sidewalls. Further microscopic cell counting indicated that ~90% of live sample cells were not stained (viable) while ~80% of dead sample cells were stained (non-viable). Combining those two populations, the overall separation efficiency of the system was estimated as ~85% at this medium conductivity [32].

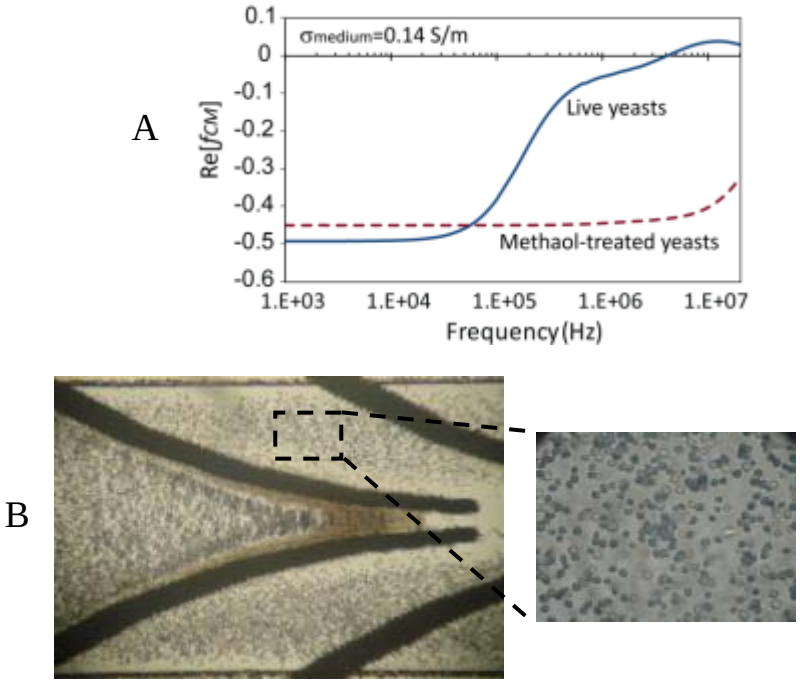

Figure 4. Separation of live and dead yeast cells using curved microelectrodes: (A) Distinct DEP response of live and dead cell, (B) Trapping of live yeasts along the microelectrodes while repelling the methanol treated (dead) ones, which are stained with Trypan blue [32].

3.4. Real-time analysis of drug-induced death of tumour cell

This work demonstrated the unique features of DEP-based microfluidic systems as promising technologies that provide a new outlook for the rapid assessment of programmed and accidental cell death and can be applied in drug discovery, high-content drug screening, and personalized clinical diagnostics [33].

Figure 5A shows the application of curved microelectrodes in an open-access configuration. In doing so, a PMMA block which accommodated two elliptical chambers was integrated onto the DEP platform. To conduct the experiments, 200 µl of human leukemic (U937) cell suspension in a LEC buffer of 0.05 S/m was injected to the PMMA chamber while the microelectrodes were energised with an AC signal of 6 V at 20 MHz [20].

Our computational model predicted that due to Joule heating effect, the activated microelectrodes will produce sufficient heat to form hot spots of 36.1°C at the tip region. This created two electro-thermal vortices within the PMMA chamber, which acted as conveyor belts, rapidly transferring the cells from all parts of the chamber towards the microelectrodes, as predicted by our computational model (Figure 4B). Once the cells were in the close proximity to the microelectrodes, they were immobilised under the increasing DEP force (Figure 4C). This created a dense layer of cells between the microelectrodes in less than 10 minutes. The magnitude of the AC signal was decreased to 4 V to minimise the side effects of exposure of cells to strong electric fields or high temperatures. Next, we injected a 20 µlit droplet of Cycloheximide drug (1.4 mg/ml) to the PMMA chamber to induce apoptosis (gradual death) of immobilised cells, and subsequently injected a 20 µlit droplet of Propidium iodide (PI, 0.25 µg/ml) a well-known indicator of plasma membrane permeability to monitor the drug-induced cell death. Addition of PI increased the average electrical conductivity of the medium to 0.25 S/m and reduced the accumulation of the remained suspended cells [20].

The immobilised cells were continuously monitored for up to 6 hours. The percentage of PI-positive (dead) cells was evaluated by merging the images of bright field and red fluorescent channels using a motorized Nikon Eclipse TiE epifluorescence microscope equipped with a cooled DS-Qi1Mc CDD camera (Figure 5C). Time-lapse data collected in 30 min intervals, as shown in Figures 6C-E. In contrast to the standard end-point analysis, our DEP platform enabled the dynamic observation of cell death in response to the cytotoxic drug. Quantification of 500 cells analysed in time intervals provided a stratified cell survival curve that did not differ from control chips without energised microelectrodes [20].

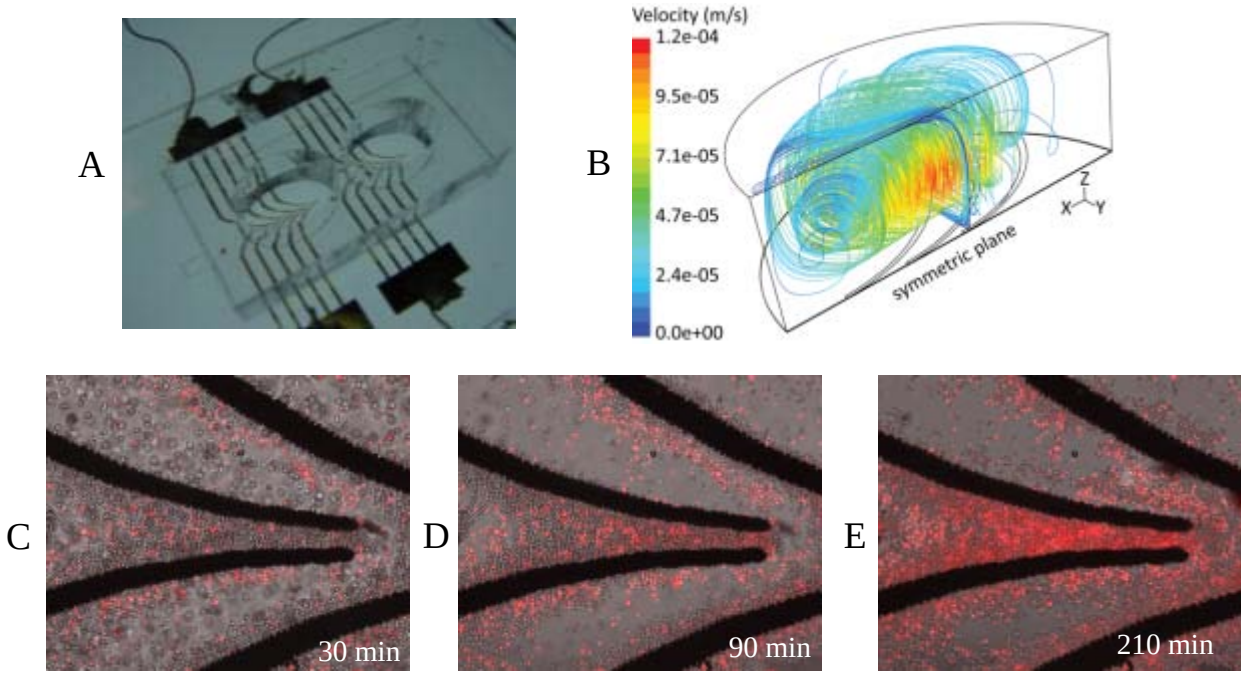

Figure 5. Real-time analysis of drug-induced cell death using curved microelectrodes: (A) The DEP device in an open-access configuration, (B) Structure of two vortices formed within the PMMA chamber, (C-E) Time-lapse imaging of trapped U937 cells stimulated with apoptosis-inducer Cycloheximide drug [20].

3.5. Interfacing tumour cells with environmental scanning electron microscopy

Suspension cells such as hematopoietic tumour cells represent a particular challenge for both the conventional and SEM imaging. Since they are non-adherent, their immobilisation during processing and analysis is hard and requires complex fixation protocols that can modify the structure, morphology, and physical-chemical properties of the cells [34].

We also applied the curved microelectrodes for environmental scanning electron microscopy (ESEM) analysis of DEP-trapped cells [35]. To immobilise the human leukemic U937 cells between the microelectrodes, the LEC buffer was initially centrifuged at 3000 rpm for 5 minutes to remove any non-dissolved particles and minimise accumulation of the colloidal residues on the surface of the cells and microelectrodes. The collected (purified) supernatant of LEC buffer was then used to wash and resuspend the cells while the conductivity of cell suspension was reduced to 0.05 S/m. To facilitate trapping, cells were exposed to the DEP field for 90-110 minutes while the microelectrodes were energised at 7.5 V and 20 MHz. Following cell immobilisation, the LEC buffer inside the chamber was gently aspirated by manual pipetting. To minimise the cell dislodgment during buffer aspiration, the pipette tip was positioned only at the periphery of the PMMA chamber and aspiration was slowly performed in 20 µl intervals. Reduction of the chamber depth to 2 mm minimised the disturbance induced by pipette suction, improving the overall stability of the immobilised cells. After buffer aspiration, the microelectrodes were de-energised and the chip containing an emulsion of the buffer was placed in a humidified atmosphere, transferred and visualised in a low vacuum mode using FEI Quanta 200 ESEM (FEG, Hillsboro, OR, USA). Figure 6 shows the high resolution ESEM imaging of the electrode tip with immobilised U937 cells [35]. Our data provide proof-of-concept that DEP immobilisation technology can be readily used to rapidly concentrate and image cells for ESEM imaging.

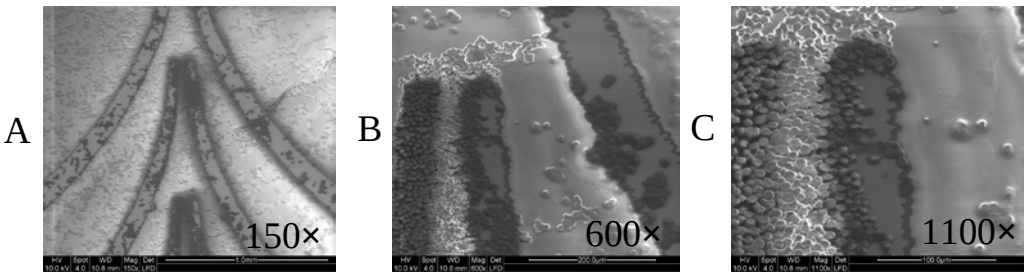

Figure 6. Proof-of-concept interfacing of the DEP cell retention and trapping technology with ESEM to provide a high-resolution analysis of individual non-adherent cells [35].

4. CONCLUSIONS

This work demonstrated the unique capabilities of curved microelectrodes to empower the DEP-based microfluidic systems. We showed that the curved microelectrodes can operate in a flow-through mode to manipulate and sort the suspended particles under the combined effect of DEP and hydrodynamic forces. Moreover, we showed that the curved microelectrodes can operate in an open-access mode to transport and immobilise the suspended particles under the combined effect of DEP and electro-hydrodynamic forces. Taking advantage of this versatility, we reported the manipulation, separation, transportation, immobilisation and characterisation of polystyrene microparticles, carbon nanotubes, yeasts and human leukemic cells for a variety of engineering and biomedical applications. Further work is needed to improve the operational characteristics of curved microelectrodes enabling them for more challenging applications. For example, the curved microelectrodes can be developed in extruded [15] or bottom-top patterned [16] configurations to produce stronger DEP force in a larger area of the micro-environment in tandem with hydrodynamic forces. Alternatively, the curved microelectrodes can be scaled down to sort and trap small bacteria or even cell organelles, or scaled up to trap and image the multi-cellular and embryonic organisms [36].

REFERENCES

[1] H. Morgan and N. G. Green, *AC Electrokinetics: colloids and nanoparticles* Baldock: Research Studies Press LTD., 2003.

[2] K. Khoshmanesh, S. Nahavandi, S. Baratchi, A. Mitchell, and K. Kalantar-zadeh, "Dielectrophoretic platforms for bio-microfluidic systems," *Biosensors & Bioelectronics,* vol. 26, pp. 1800-1814, Jan 15 2011.

[3] B. Cetin and D. Li, "Dielectrophoresis in microfluidics technology," *Electrophoresis,* vol. 32, pp. 2410-2427, 2011.

[4] Y. Kang and D. Li, "Electrokinetic motion of particles and cells in microchannels," *Microfluidics and Nanofluidics,* vol. 6, pp. 431-460, 2009.

[5] T. B. Jones, M. Gunji, M. Washizu, and M. J. Feldman, "Dielectrophoretic liquid actuation and nanodroplet formation," *Journal of Applied Physics,* vol. 89, pp. 1441-1448, 2001.

[6] M. D. Pysher and M. A. Hayes, "Electrophoretic and dielectrophoretic field gradient technique for separating bioparticles," *Analytical Chemistry,* vol. 79, pp. 4552-4557, Jun 2007.

[7] P. R. C. Gascoyne and J. V. Vykoukal, "Dielectrophoresis-based sample handling in general-purpose programmable diagnostic instruments," *Proceedings of the IEEE,* vol. 92, pp. 22-42, Jan 2004.

[8] P. R. C. Gascoyne, J. Noshari, T. J. Anderson, and F. F. Becker, "Isolation of rare cells from cell mixtures by dielectrophoresis," *Electrophoresis,* vol. 30, pp. 1388-1398, Apr 2009.

[9] W. M. Arnold and N. R. Franich, "Cell isolation and growth in electric-field defined micro-wells," *Current Applied Physics,* vol. 6, pp. 371-374, Jun 2006.

[10] M. S. Pommer, Y. T. Zhang, N. Keerthi, D. Chen, J. A. Thomson, C. D. Meinhart, and H. T. Soh, "Dielectrophoretic separation of platelets from diluted whole blood in microfluidic channels," *Electrophoresis,* vol. 29, pp. 1213-1218, Mar 2008.

[11] K. Khoshmanesh, C. Zhang, F. J. Tovar-Lopez, S. Nahavandi, S. Baratchi, K. Kalantar-Zadeh, and A. Mitchell, "Dielectrophoretic manipulation and separation of microparticles using curved microelectrodes," *Electrophoresis,* vol. 30, pp. 3707-3717, Nov 2009.

[12] F. Grom, J. Kentsch, T. Muller, T. Schnelle, and M. Stelzle, "Accumulation and trapping of hepatitis A virus particles by electrohydrodynamic flow and dielectrophoresis," *Electrophoresis,* vol. 27, pp. 1386-1393, Apr 2006.

[13] A. Rosenthal and J. Voldman, "Dielectrophoretic Traps for Single-Particle Patterning," *Biophysical Journal,* vol. 88, pp. 2193-2205, 2005.

[14] R. S. Thomas, H. Morgan, and N. G. Green, "Negative DEP traps for single cell immobilisation," *Lab on a Chip,* vol. 9, pp. 1534-1540, 2009.

[15] J. Voldman, M. L. Gray, M. Toner, and M. A. Schmidt, "A microfabrication-based dynamic array cytometer," *Analytical Chemistry,* vol. 74, pp. 3984-3990, Aug 2002.

[16] M. Durr, J. Kentsch, T. Muller, T. Schnelle, and M. Stelzle, "Microdevices for manipulation and accumulation of micro- and nanoparticles by dielectrophoresis," *Electrophoresis,* vol. 24, pp. 722-731, Feb 2003.

[17] L. Wang, L. A. Flanagan, N. L. Jeon, E. Monuki, and A. P. Lee, "Dielectrophoresis switching with vertical sidewall electrodes for microfluidic flow cytometry," *Lab on a Chip,* vol. 7, pp. 1114-1120, 2007.

[18] B. H. Lapizco-Encinas, B. A. Simmons, E. B. Cummings, and Y. Fintschenko, "Insulator-based dielectrophoresis for the selective concentration and separation of live bacteria in water," *Electrophoresis,* vol. 25, pp. 1695-1704, Jun 2004.

[19] H. Shafiee, J. L. Caldwell, M. B. Sano, and R. V. Davalos, "Contactless dielectrophoresis: a new technique for cell manipulation," *Biomedical Microdevices,* vol. 11, pp. 997-1006, Oct 2009.

[20] K. Khoshmanesh, J. Akagi, S. Nahavandi, J. Skommer, S. Baratchi, J. M. Cooper, K. Kalantar-Zadeh, D. E. Williams, and D. Wlodkowic, "Dynamic Analysis of Drug-Induced Cytotoxicity Using Chip-Based Dielectrophoretic Cell Immobilization Technology," *Analytical Chemistry,* vol. 83, pp. 2133-2144, Mar 15 2011.

[21] K. Khoshmanesh, C. Zhang, S. Nahavandi, F. J. Tovar-Lopez, S. Baratchi, A. Mitchell, and K. Kalantar-Zadeh, "Size based separation of microparticles using a dielectrophoretic activated system," *Journal of Applied Physics,* vol. 108, Aug 1 2010.

[22] K. Kalantar-zadeh, K. Khoshmanesh, A. A. Kayani, S. Nahavandi, and A. Mitchell, "Dielectrophoretically tuneable optical waveguides using nanoparticles in microfluidics," *Applied Physics Letter* vol. 96, p. 101108 2010.

[23] A. A. Kayani, C. Zhang, K. Khoshmanesh, J. L. Campbell, A. Mitchell, and K. Kalantar-zadeh, "Novel tuneable optical elements based on nanoparticle suspensions in microfluidics," *Electrophoresis,* vol. 31, pp. 1071-1079, 2010.

[24] A. F. Chrimes, A. A. Kayani, K. Khoshmanesh, P. R. Stoddart, P. Mulvaney, A. Mitchell, and K. Kalantar-Zadeh, "Dielectrophoresis-Raman spectroscopy system for analysing suspended nanoparticles," *Lab on a Chip,* vol. 11, pp. 921-928, 2011.

[25] K. Khoshmanesh, C. Zhang, S. NahavandI, F. J. Tovar-Lopez, S. Baratchi, Z. Hu, A. Mitchell, and K. Kalantar-zadeh, "Particle trapping using dielectrophoretically patterned carbon nanotubes," *Electrophoresis,* vol. 31, pp. 1-10, 2010.

[26] D. Gänshirt, F. W. M. Smeets, A. Dohr, C. Walde, I. Steen, C. Lapucci, C. Falcinelli, R. Sant, M. Velasco, H. S. P. Garritsen, and W. Holzgreve, "Enrichment of fetal nucleated red blood cells from the maternal circulation for prenatal diagnosis experiences with triple density gradient and MACS based on more than 600 cases," *Fetal Diagnosis and Therapy,* vol. 13, pp. 276-286, 1998.

[27] H. Hatanaka, T. Yasukawa, and F. Mizutani, "Detection of surface antigens on living cells through incorporation of immunorecognition into the distinct positioning of cells with positive and negative dielectrophoresis," *Analytical Chemistry,* vol. 83, pp. 7207-7212, 2011.

[28] H. Yang, H. Li, and X. Jiang, "Detection of foodborne pathogens using bioconjugated nanomaterials," *Microfluidics and Nanofluidics,* vol. 5, pp. 571-583, 2008.

[29] D. Wlodkowic and J. M. Cooper, "Tumors on chips: Oncology meets microfluidics," *Current Opinion in Chemical Biology,* vol. 14, pp. 556-567, 2010.

[30] S. Sergent-Tanguy, C. Chagneau, I. Neveu, and P. Naveilhan, "Fluorescent activated cell sorting (FACS): A rapid and reliable method to estimate the number of neurons in a mixed population," *Journal of Neuroscience Methods,* vol. 129, pp. 73-79, 2003.

[31] N. Modak, A. Datta, and R. Ganguly, "Cell separation in a microfluidic channel using magnetic microspheres," *Microfluidics and Nanofluidics,* vol. 6, pp. 647-660, 2009.

[32] K. Khoshmanesh, C. Zhang, F. J. Tovar-Lopez, S. Nahavandi, S. Baratchi, K. Kalantar-Zadeh, and A. Mitchell, "Dielectrophoretic-activated cell sorter based on curved microelectrodes," *Microfluidics and Nanofluidics,* vol. Online, pp. DOI 10.1007/s10404-009-0558-7, 2010.

[33] D. Wlodkowic, K. Khoshmanesh, J. C. Sharpe, Z. Darzynkiewicz, and J. M. Cooper, "Apoptosis goes on a chip: advances in the microfluidic analysis of programmed cell death," *Analytical Chemistry,* vol. 83, pp. 6439-6446, Sep 1 2011.

[34] D. Wlodkowic, S. Faley, M. Zagnoni, J. P. Wikswo, and J. M. Cooper, "Microfluidic Single-Cell Array Cytometry for the Analysis of Tumor Apoptosis," *Analytical Chemistry,* vol. 81, pp. 5517-5523, Jul 1 2009.

[35] K. Khoshmanesh, J. Akagi, S. Nahavandi, K. Kalantar-zadeh, S. Baratchi, D. E. Williams, J. M. Cooper, and D. Wlodkowic, "Interfacing Cell-Based Assays in Environmental Scanning Electron Microscopy Using Dielectrophoresis," *Analytical Chemistry,* vol. 83, pp. 3217-3221, Apr 15 2011.

[36] K. Khoshmanesh, N. Kiss, S. Nahavandi, C. W. Evans, J. M. Cooper, D. E. Williams, and D. Wlodkowic, "Trapping and imaging of micron-sized embryos using dielectrophoresis," *Electrophoresis,* pp. n/a-n/a, 2011.